The neuroimmune guidance cue netrin-1 promotes atherosclerosis by inhibiting the emigration of macrophages from plaques

Published in final edited form as:
Nat Immunol. ; 13(2): 136–143. doi:10.1038/ni.2205.

The neuroimmune guidance cue netrin-1 promotes atherosclerosis by inhibiting macrophage emigration from plaques

Janine M van Gils[1], **Merran C Derby**[2], **Luciana R Fernandes**[3], **Bhama Ramkhelawon**[1], **Tathagat D Ray**[1], **Katey J Rayner**[1], **Sajesh Parathath**[1], **Emilie Distel**[1], **Jessica L Feig**[1], **Jacqueline I Alvarez-Leite**[3], **Alistair J Rayner**[1], **Thomas O McDonald**[4], **Kevin D O'Brien**[4], **Lynda M Stuart**[5], **Edward A Fisher**[1,6], **Adam Lacy-Hulbert**[5], and **Kathryn J Moore**[1,6]

[1]Marc and Ruti Bell Vascular Biology and Disease Program, Leon H. Charney Division of Cardiology, Department of Medicine, New York University School of Medicine, New York, NY, USA

[2]Department of Medicine, Massachusetts General Hospital, Harvard Medical School, Boston, MA, USA

[3]Department of Biochemistry and Immunology, Federal University of Minas Gerais, Belo Horizonte, MG, Brazil

[4]Division of Cardiology, University of Washington, Seattle, WA, USA

[5]Department of Pediatrics, Program for Developmental Immunology, Massachusetts General Hospital, Harvard Medical School, Boston, MA, USA

[6]Department of Cell Biology, New York University School of Medicine, New York, NY, USA

Abstract

Atherosclerotic plaque formation is fueled by the persistence of lipid-laden macrophages in the artery wall. The mechanisms by which these cells become trapped, thereby establishing chronic inflammation, remain unknown. Netrin-1, a neuroimmune guidance cue, was secreted by macrophages in human and mouse atheroma, where it inactivated macrophage migration to chemokines implicated in their egress from plaques. Acting via its receptor UNC5b, netrin-1 inhibited CCL2- and CCL19-directed macrophage migration, Rac1 activation and actin polymerization. Targeted deletion of netrin-1 in macrophagesseverely diminished atherosclerosis progression in $Ldlr^{-/-}$ mice and promoted macrophage emigration from plaques. Thus, netrin-1 promotes atherosclerosis by retaining macrophages in the artery wall and establish a causative role for negative regulators of leukocyte migration in chronic inflammation.

Atherosclerosis is a disease of chronic inflammation that is distinguished by the persistence of cholesterol-engorged macrophages in arterial plaques. Arterial inflammation is initiated by the subendothelial retention of plasma low density lipoprotein (LDL), and enhanced by

Correspondence should be addressed to K.J.M. (kathryn.moore@nyumc.org), Kathryn J. Moore, Ph.D., New York University School of Medicine, 522 First Avenue, Smilow 705, New York, NY 10016, tel: 212.263.9259, fax: 212.263.9115.

AUTHOR CONTRIBUTIONS

J.vG. performed migration and atherosclerosis studies; M.D. performed smooth muscle studies and fetal liver cell transplantation; K.R and L.F. performed mouse atherosclerosis studies, J.A-L., S.P. and B.R. performed microscopy; T.R., A.R. and J.F performed biochemical assays; T.M. and K.O. performed immunohistochemical studies of human atheroma; E.D. and E.F. assisted in bead labeling experiments, L.S and A.L-H. contributed to experimental design, data analysis and provided helpful discussion; K.M. designed, analyzed and interpreted the studies and wrote the manuscript with J.vG. The authors have no competing financial interests.

oxidative modification of these lipoproteins, which triggers an influx of monocytes[1]. Unlike other inflammatory states, atherosclerotic inflammation does not readily resolve and cholesterol-laden macrophages persist in the arterial wall. These macrophage “foam cells” cause expansion of the plaque though recruitment of additional leukocytes and vascular smooth muscle cells, and contribute prominently to plaque instability through the secretion of extracellular matrix-degrading proteases and cytotoxic factors. Notably, atherosclerotic plaques that cause clinical events (ie. myocardial infarction and stroke) are characterized by a high macrophage content[2].

While macrophage retention in the artery wall has long been recognized as a fundamental step in creating the chronic inflammatory milieu underlying atherosclerosis, the mechanisms regulating this process are not well understood. Resolution of acute inflammation typically involves emigration of monocyte-derived cells out of the inflamed site through nearby lymphatic vessels[3]. This process appears to be impaired in atherosclerosis and has been attributed, in part, to the cholesterol loading of macrophages which shifts these cells to a more sessile phenotype[4]. Recent studies in transplant-based mouse models of atherosclerosis regression have shown that reducing plasma non-HDL cholesterol and/or increasing high-density lipoproteins (HDL), promotes emigration of macrophages from lesions to regional and systemic lymph nodes[5-9]. Macrophage expression of the chemokine receptor CCR7 was shown to be essential for decreasing the macrophage content of plaques[8,9], implicating the CCR7-specific ligands CCL19 and CCL21 in promoting the egress of these cells from the artery wall. These studies indicate that macrophage emigration from the plaque is actively inhibited during hypercholesterolemia, although the regulatory signals that impair this process remain largely unknown.

A paradigm for inhibitory guidance cues exists in the developing nervous system, where axonal migration relies on the integration of both chemorepulsive and chemoattractive signals to steer the axonal growth cone. One such guidance molecule netrin-1, a secreted laminin-related molecule, mediates both chemorepulsion and chemoattraction of axons navigating the spinal cord midline. This context-dependent response to netrin-1 is regulated by differential receptor expression by the target cell. For example, neurons expressing the Deleted in Colon Cancer (DCC) receptor or Neogenin are attracted by a diffusible gradient of netrin-1 secreted at the midline[10]. Conversely, co-expression of the UNC5b receptor with DCC converts netrin-1 attraction to repulsion, whereas expression of UNC5b alone mediates short-range repulsion[10,11]. Previous studies have uncovered instructional roles for netrin-1 and its receptors outside the nervous system in organogenesis[12,13], angiogenesis[14,15] and tumorigenesis[16,17], suggesting that netrin-1 regulates cell migration in a broader context.

Work from our group identified netrin-1 as a leukocyte guidance cue expressed by the endothelium that is downregulated during acute infection with *Staphylococcus aureus*[18]. These studies established that netrin-1 inhibited migration of monocytes, neutrophils and lymphocytes via its receptor UNC5b. Recent studies in models of hypoxia and reperfusion injury have extended these findings to show that expression of netrin-1 by epithelial cells also attenuates leukocyte accumulation[18-21]. Given its role in inhibiting leukocyte migration, we sought to determine whether netrin-1 contributed to the retention of macrophages in the chronic inflammatory milieu of the atherosclerotic plaque. Our studies show that netrin-1 was abundantly expressed by macrophage foam cells formed *in vitro* and *in vivo*, and in atherosclerotic lesions. In functional studies we demonstrate that netrin-1 expressed by foam cells differentially regulated the cellular constituents of atheroma. Netrin-1 inactivated macrophage migration and supported chemoattraction of coronary artery smooth muscle cells. Thus, expression of netrin-1 in plaques would be predicted to simultaneously prevent inflammatory cell egress and induce smooth muscle cell recruitment into the intima, thereby promoting lesion progression. In support of thishypothesis, we demonstrate that deletion of

netrin-1 in myeloid cells severely reduced atherosclerosis lesion size and complexity in *Ldlr*$^{-/-}$ mice and was associated with macrophage emigration from plaques.

RESULTS

Macrophage foam cells express the guidance cue netrin-1

Given its role in attenuating leukocyte migration[18], we first investigated whether netrin-1 is expressed in atherosclerotic plaques. Immunostaining of serial sections of human coronary artery atherosclerotic plaques showed expression of netrin-1 and its chemorepulsive receptor UNC5H2 (also called UNC5b) in lesional cells that express the macrophage marker HAM56 (Supplementary Fig 1a,b). By contrast, DCC, the chemoattractive netrin-1 receptor, was not detected in these plaques (data not shown). A similar pattern of lesional netrin-1 staining was seen in the *Ldlr*$^{-/-}$ mouse model of atherosclerosis (Fig. 1a). In aortic sinus plaques of *Ldlr*$^{-/-}$ mice fed a western diet (WD) for 12 weeks, double staining for netrin-1 and the macrophage marker CD68 showed netrin-1 expression by lesional macrophages. In addition, extracellular netrin-1 staining was apparent in macrophage-rich regions of the plaque, consistent with netrin-1 being a secreted protein that can bind to extracellular matrix components. Analysis of the aortic arch, a second site of lesion predilection in mice, showed that *Ntn1* mRNA was increased in *Ldlr*$^{-/-}$ mice compared to wild-type C57BL/6 mice, and netrin-1 expression was further upregulated by feeding these mice a WD (Fig. 1b). Similar results were obtained in the *Apoe*$^{-/-}$ mouse model of atherosclerosis (Supplementary Fig. 1c), indicating that netrin-1 expression by lesional macrophages is a common characteristic of mouse and human atheroma.

To understand the molecular mechanisms regulating netrin-1 and UNC5b expression, we isolated peritoneal macrophages (pMø) from *Ldlr*$^{-/-}$ mice fed either a chow or WD. In this commonly used model of *in vivo* foam cell formation, WD-feeding markedly increased *Ntn1* and *Unc5b* mRNAs, whereas expression of CD68 was unchanged (Fig. 1c). Similar results were observed in hypercholesterolemic *Apoe*$^{-/-}$ mice (Supplementary Fig. 1d), suggesting that increased cellular lipid accumulation may upregulate expression of netrin-1 and UNC5b. To test this, we treated pMø with native LDL, or LDL that had been oxidized (oxLDL), a modification that promotes cholesterol loading of macrophages.

Consistent with our *in vivo* data, oxLDL, but not LDL, increased macrophage expression of *Ntn1* and *Unc5b* mRNA (Fig. 1d, Supplementary Fig. 1e). Immunoblot analysis confirmed increased cell-associated netrin-1 protein in oxLDL-treated macrophages (Fig. 1e), which was paralleled by an increase in netrin-1 in cell culture supernatants (Fig. 1f). Notably, the induction of *Ntn1* mRNA (Fig. 1g) and netrin-1 protein (Supplementary Fig. 1f) by oxLDL required CD36, a scavenger receptor previously implicated in macrophage retention in atherosclerotic plaques[22]. Because we and others have shown that oxLDL binding to CD36 induces NF-κB activation[23,24] and the *Ntn1* promoter contains an NF-κB binding site[20], we investigated whether NF-κB contributes to the upregulation of *Ntn1*. Using a *Ntn1* promoter-luciferase reporter gene, we demonstrate that *Ntn1* promoter activity was induced by oxLDL and this was reduced by the NF-κB inhibitor BAY 11-7082 (Fig. 1h). Collectively, these data demonstrate that loading of macrophages with cholesterol under physiologic conditions, or by oxidized lipids via CD36 *in vitro*, increases expression of netrin-1 and its receptor UNC5b.

Netrin-1 blocks the directed migration of macrophages

We next assessed the impact of netrin-1 on macrophage chemotaxis using transwell Boyden chambers and a real-time detection method (xCelligence). Using both methods, recombinant netrin-1 potently inhibited the chemotaxis of the macrophage cell line RAW264.7 to CCL2,

also known as monocyte chemoattractant protein-1 (MCP-1), but had little effect on macrophage migration in the absence of chemokine (Fig. 2a-b). The inhibitory effects of netrin-1 on chemotaxis were dose dependent (Fig. 2a), with 250 ng/ml netrin-1 inhibiting CCL2-induced migration by >90% (Fig. 2b). Furthermore, pre-treating RAW264.7 cells with netrin-1 for 1 h rendered the cells refractory to CCL2 (Fig 2c). Similar to its effects on RAW264.7 macrophages, netrin-1 potently inhibited chemotaxis of pMø to CCL2 (Fig 2d). This effect was not chemokine-specific, as netrin-1 also blocked migration of RAW264.7 and pMø to the CCR7 ligands CCL19 and CCL21 (Fig 2e, Supplemental Fig. 2a-g), chemokines implicated in the egress of $CD68^+$ cells from plaques[8,9]. To gain insight into the mechanisms by which netrin-1 inhibits macrophage chemotaxis, we measured its effect on organization of the actin cytoskeleton. Stimulation of pMø with CCL2 or CCL19 induced a marked reorganization of actin, characterized by the appearance of membrane ruffles, lamellipodia and filapodia (Fig. 2f (arrows), Supplementary Fig. 3a), and rapid cell spreading (Fig. 2g, Supplementary Fig. 3b). By contrast, pMø pre-treated withnetrin-1 prior to stimulation with CCL2 or CCL19 maintained a rounded morphology (Fig. 2f (arrowheads), Supplementary Fig. 3a) and showed no increase in mean cell area (Fig. 2g, Supplementary Fig. 3b), consistent with a non-motile status. Quantification of phalloidin-stained actin filaments by flow cytometry confirmed that netrin-1 blocked the increase in polymerized actin-1 associated with CCL2 stimulation (Fig. 2h). As the Rho GTPase Rac1 plays a key role in the reorganization of actin in macrophages, we next investigated whether netrin-1 altered Rac1 activation following chemotactic stimulation using glutathione-S-transferase (GST) beads conjugated to the PAK1-PBD to detect the activated GTP-bound form of Rac1. Whereas netrin-1 pretreatment of macrophages modestly increased basal amounts of activated Rac1, it inhibited CCL2-induced Rac1 activation (Fig. 2i) and phosphorylation of the focal adhesion kinase FAK (Fig. 2j), which cooperates with Rac1 to link the actin cytoskeleton to the extracellular matrix during cell spreading and migration. Collectively, these data indicate that netrin-1 inhibits the directional migration of macrophages by disrupting the Rac1 signaling cascade, re-organization of the actin cytoskeleton and cell polarization. As both netrin-1 and UNC5b were upregulated in cholesterol-loaded macrophages we postulated that netrin-1 secreted by macrophages in atherosclerotic plaques may act in an autocrine or paracrine manner via UNC5b to immobilize these cells in the artery wall. To test the role of UNC5b in the response to netrin-1, we pre-incubated macrophages with a recombinant UNC5b-Fc fusion protein or an antibody that binds to the extracellular domain of UNC5b. Both the recombinant UNC5b-Fc (Fig. 3a) and Unc5b antibody (Fig. 3b), but not control IgG, reversed the inhibitory effect of netrin-1 on CCL19-induced migration. By contrast, no change was seen with an inhibitor of the A2B adenosine receptor, another netrin-1 receptor implicated in the attenuation of neutrophil migration (Fig. 3c). Furthermore, consistent with the secretion of netrin-1 by macrophage foam cells, conditioned medium from oxLDL-but not LDL-treated macrophages, inhibited cell migration to CCL19 (Fig. 3d), and this was reversed by recombinant UNC5b-Fc (Fig. 3e). To confirm that netrin-1 is the active component secreted by oxLDL-treated Mø, we used pMø isolated from $Ntn1^{-/-}$ bone marrow chimeric mice, which do not express netrin-1 in response to oxLDL (Fig. 3f). Whereas conditioned medium from oxLDL-treated $Ntn1^{+/+}$ pMø inhibits migration of naïve macrophages to CCL19 by 80%, conditioned medium from similarly treated $Ntn1^{-/-}$ macrophages reduces migration by only 25% (Fig. 3f). Furthermore, $Ntn1^{+/+}$ conditioned medium incubated with recombinant UNC5b-Fc inhibited migration to a similar extent as $Ntn1^{-/-}$ conditioned medium (≈25%). By contrast, the effects of $Ntn1^{-/-}$ conditioned medium were unchanged by the addition of recombinant UNC5b (Fig. 3f). Together, these data suggest that netrin-1 secreted by cholesterol-laden macrophages would promote their accumulation in atherosclerotic plaques by inhibiting their emigration from this site of inflammation.

Studies in a transplant mouse model of atherosclerosis regression have demonstrated that macrophages in plaques exit via nearby lymphatics upon aggressive cholesterol lowering[6]. A similar pathway for macrophage clearance has been reported during resolving peritonitis where inflammatory macrophages emigrate to the draining lymphatics of the omentum[3,25]. To test the effect of netrin-1 on macrophage emigration *in vivo* we used a well-characterized thioglycollate-induced peritonitis model in which administration of lipopolysaccharide (LPS) induces the rapid egress of recruited leukocytes from the peritoneum[22]. As previously reported, *i.p.* injection of LPS reduced the number of leukocytes in the peritoneum by 75% in control mice (Fig. 3g). By contrast, mice pretreated with netrin-1 (i.p.) 45 min prior to this inflammatory stimulus showed no significant change in peritoneal leukocytes. Flow cytometric analysis of the macrophage marker F4/80 confirmed that macrophages were retained in the peritoneum of netrin-1 pre-treated mice compared to control mice ($0.4 \times 10^6 \pm 0.1 \times 10^6$ control vs. $1.1 \times 10^6 \pm 0.3 \times 10^6$ netrin-1). These data demonstrate that netrin-1 can inhibit the emigration of macrophages from a site of active inflammation.

Netrin-1 is a chemoattractant for smooth muscle cells

During the progression of atherosclerosis, smooth muscle cells from the underlying medial layer are recruited to the plaque and participate in promoting plaque growth. To investigate whether netrin-1 expression in plaque affects other cellular components of the atherosclerotic lesion, we measured its effect on migration of human coronary artery smooth muscle cells (CaSMCs). Unlike its inhibitory effect on macrophages, netrin-1 dose-dependently induces migration of CaSMCs (Fig. 4a). Furthermore, conditioned medium from oxLDL-, but not LDL-treated macrophages induces migration of CaSMCs (Fig. 4b). To understand how Netrin-1 mediates chemoattraction of CaSMCs, we measured expression of its known receptors. Whereas CaSMCs had low expression of *Dcc* and *Unc5b*, these cells abundantly expressed the DCC-related receptor neogenin (Fig. 4c-d), as previously reported for vascular smooth muscle cells[13]. Notably, pre-treatment of CaSMCs with a neogenin antibody abrogated the chemoattractive effect of conditioned medium from oxLDL-treated macrophages (Fig. 4e), supporting a role for foam cell derived netrin-1 in inducing SMC migration. Immunohistochemical staining of atherosclerotic plaques of $Ldlr^{-/-}$ mice showed colocalization of neogenin with smooth muscle actin (Fig. 4f), but not the macrophage marker CD68 (Supplementary Fig. 4a). Furthermore, neogenin was expressed in medial smooth muscle cells (arrows) and in smooth muscle cells that had migrated into the intima (arrowheads), as well as some cells that were not smooth muscle actin positive (Fig. 4f). Together these data indicate that through distinct mechanisms netrin-1 modulates CaSMC and macrophages migration.

Hematopoietic deficiency of netrin-1 reduces atherosclerosis

Based on the above data we postulated that expression of netrin-1 by macrophage foam cells may promote atherosclerotic plaque growth by both blocking macrophage egress and inciting smooth muscle cell recruitment in the intima. To test this hypothesis, we used fetal liver cells from day E14 $Ntn1^{-/-}$ or $Ntn1^{+/+}$ (WT) pups to reconstitute the bone marrow of lethally irradiated $Ldlr^{-/-}$ mice, thereby generating $Ldlr^{-/-}$ mice with either $Ntn1^{-/-}$ or WT macrophages. Four weeks post-transplantation, the chimeric $Ntn1^{-/-} \rightarrow Ldlr^{-/-}$ and $WT \rightarrow Ldlr^{-/-}$ mice were challenged with a WD for 12 weeks. Analysis of *Ntn1* and *Ldlr* gene expression in both circulating leukocytes and pMø of recipient mice confirmed a complete change in the genotype to the donor types (Supplementary Table 1, Supplementary Fig. 4b). There were no differences in serum total cholesterol and triglyceride concentrations, or cholesterol distribution in VLDL, LDL, and HDL in chimeric $Ntn1^{-/-} \rightarrow Ldlr^{-/-}$ and $WT \rightarrow Ldlr^{-/-}$ mice (Supplementary Table 1, Supplementary Fig. 4c). Despite these similar serum cholesterol profiles, $Ldlr^{-/-}$ mice lacking expression of *Ntn1* in bone marrow-derived cells show a striking reduction in atherosclerosis (Fig. 5).

Analysis of the aorta en face showed that *Ntn1*$^{-/-}$ →*Ldlr*$^{-/-}$ mice had a 55% reduction in mean atherosclerotic lesion area compared to *WT*→*Ldlr*$^{-/-}$ mice (Fig 5a) that was present throughout the aorta (Supplemental Fig. 4d). Isolation of mRNA from the aortic arch of the *Ntn1*$^{-/-}$ →*Ldlr*$^{-/-}$ mice showed reduced expression of the macrophage marker CD68 compared to *WT*→*Ldlr*$^{-/-}$ mice (Fig. 5b), and correspondingly, lower expression of *Ntn1* (Fig. 5c). *Ntn1*$^{-/-}$ →*Ldlr*$^{-/-}$ mice also had reduced expression of markers for other leukocyte subsets in the aortic arch, including CD3 (T cell) and CD11c (dendritic cell) (Fig. 5b). Furthermore, analysis of atherosclerotic plaques in a second anatomical site, the aortic root, showed markedly smaller lesion area in *Ntn1*$^{-/-}$ →*Ldlr*$^{-/-}$ mice compared to *WT* →*Ldlr*$^{-/-}$ mice (Fig. 5d-f). Quantification of lesion burden by cross-sectional analysis of the aortic root established that this decrease in lesion area in *Ntn1*$^{-/-}$ →*Ldlr*$^{-/-}$ mice was consistently present throughout the 400 μm of the aortic root (Fig. 5e).

Histological characterization of the aortic sinus plaques using the Stary method revealed that *WT*→*Ldlr*$^{-/-}$ mice had more advanced atherosclerosis, typified by a greater proportion of complex lesions (stage 3-4), whereas *Ntn1*$^{-/-}$ →*Ldlr*$^{-/-}$ plaques tended to be less progressed (stage 1-3) (Fig. 6a). Immunohistochemical staining of aortic sinus plaques confirmed a reduction in both macrophage (MOMA-2, Fig. 6b) and smooth muscle cells (alpha smooth muscle actin, Fig. 6c) in *Ntn1*$^{-/-}$ →*Ldlr*$^{-/-}$ compared to *WT*→*Ldlr*$^{-/-}$ mice. During the progression of atherosclerosis, macrophage persistence contributes to changes in plaque morphology, particularly the formation of the necrotic core. This critical feature of dangerous plaques arises from the combination of apoptosis of cholesterol-laden macrophages and defective phagocytic clearance of the apoptotic cells by the surrounding macrophages (efferocytosis). Notably, TUNEL staining revealed that plaques in *Ntn1*$^{-/-}$ →*Ldlr*$^{-/-}$ mice contained significantly fewer apoptotic cells compared to *WT*→*Ldlr*$^{-/-}$ mice (Fig. 6d) and this correlated with a 46% decrease in necrotic area in *Ntn1*$^{-/-}$ →*Ldlr*$^{-/-}$ plaques (Fig. 6e). Together these data suggest that netrin-1 expression by lesional macrophages promotes atherosclerotic plaque growth and complexity by enhancing macrophage retention in the intima.

To test whether netrin-1 expression in plaques inhibits macrophage emigration, we used a macrophage tracking technique in which monocytes can be selectively labeled *in vivo* with fluorescent beads so that their movement into[26] and out of[7] plaques can be tracked. *WT* →*Ldlr*$^{-/-}$ and *Ntn1*$^{-/-}$ →*Ldlr*$^{-/-}$ mice were harvested 72 h after labeled bead injection, a time point previously shown to have peak recruitment of labeled cells to atherosclerotic plaque ("baseline")[26], and after 14 days to measure the number of labeled macrophages remaining in plaques. The number of bead-labeled macrophages in *WT*→*Ldlr*$^{-/-}$ plaques was similar at baseline and 14 days, indicating that macrophages did not emigrate during this time (Fig. 6f). By contrast, in *Ntn1*$^{-/-}$ →*Ldlr*$^{-/-}$ plaques there was a 40% decrease in beads after 14 days compared to baseline, indicating that fewer macrophages were retained in the plaque in the absence of netrin-1. As the beads cannot be degraded, and any labeled macrophages undergoing apoptosis are phagocytosed by surrounding macrophages thereby transferring the bead label, the reduction in beads in the *Ntn1*$^{-/-}$ →*Ldlr*$^{-/-}$ mice was indicative of macrophage movement out of the plaque. Collectively, our data support the retention of macrophages in plaques by netrin-1 and demonstrate that upon the removal of this retention signal, macrophages emigrate from this site of chronic inflammation.

DISCUSSION

It is appreciated that plaques that cause clinical events, so called "vulnerable plaques", have a high macrophage content[2]. Thus, strategies targeted at reducing macrophage accumulation and/or directing emigration of these cells from the plaque offer promise as a complement to standard lipid lowering therapies. However to date, the signals responsible for mediating

macrophage retention in the artery wall have been poorly understood. Our data establish that netrin-1, a neuronal guidance molecule with recently ascribed immunomodulatory functions, and its receptor UNC5b, are expressed by macrophage foam cells of human and mouse atherosclerotic plaques. Notably, recombinant netrin-1 and netrin-1 secreted by *in vitro* formed foam cells potently block the directed migration of macrophages to CCL19, a chemokine implicated in the emigration of monocyte-derived cells from plaques in a transplant model of regression[8,9]. Moreover, netrin-1 also blocked migration of macrophages to CCL2, which along with its receptor CCR2, has been shown to play roles in myeloid cell trafficking to the lymph node during inflammation[27,28]. Thus, netrin-1 in plaques may act to immobilize macrophage foam cells and prevent their egress to the lumen or lymphatic system. Supporting this hypothesis, we find that the selective deletion of netrin-1 in bone marrow derived cells markedly reduces atherosclerotic lesion size and complexity in $Ldlr^{-/-}$ mice, and is associated with macrophage emigration from plaques. These data establish a causative role for netrin-1 in the persistence of inflammation in atherosclerosis, and highlight the importance of such negative regulators of leukocyte migration in chronic inflammation.

There have been an increasing number of reports that guidance molecules characterized in the developing nervous system can modulate leukocyte migration in inflammatory states[18,29-31]. Such studies have shown that members of the netrin, slit, semaphorin and ephrin families of guidance cues can have both chemoattractive and chemorepulsive effects on leukocyte trafficking. Recent studies from our group and others have shown that netrin-1 is expressed on endothelial and epithelial cells, where it appears to function in limiting leukocyte transmigration into tissues[18-20,32]. For example, endothelial expression of netrin-1 is downregulated in the lung during acute *Staphylococcus aureus* induced inflammation, coincident with recruitment of neutrophils to the tissue[18]. By contrast, netrin-1 is upregulated on gut epithelial cells during transient ischemia and attenuates neutrophil recruitment to protect from hypoxia-induced inflammation[20]. These studies showing that netrin-1 inhibits migration of circulating leukocytes into tissues, and thus is anti-inflammatory in this capacity, have provided insight into the homeostatic barrier functions performed by netrin-1. In this regard, a recent study reported that intravenous viral delivery of netrin-1 to $Ldlr^{-/-}$ mice reduced atherosclerosis[33], presumably by increasing its expression on endothelial cells, although no determination of the cell types expressing netrin-1 were made. Unfortunately, this study was underpowered and the traditional atherosclerosis measurements of cross-sectional lesion area and en face aortic lesion burden were not assessed, limiting its conclusions. By contrast, our data indicate that the expression of netrin-1 by macrophage foam cells within plaques is pro-atherosclerotic, and its inactivation of macrophage emigration from this inflamed site likely inhibits the resolution of inflammation. Thus, as in the nervous system where netrin-1 can have both positive and negative effects on axonal migration, it may play multifunctional roles in regulating inflammation depending on the site of its expression.

While expressed at low levels in monocytes and most tissue macrophages, netrin-1 is highly expressed by macrophage foam cells in human and mouse atheroma. The mechanisms of netrin-1 upregulation in this context may be similar to those in hypoxia, where HIF1-α and NF-κB regulate netrin-1 transcription[19,20,34]. Hypoxic stress is intimately linked to atherosclerosis[35] and these transcription factors are activated in lesional macrophage. Induction of netrin-1 by oxLDL involved activation of NF-κB via CD36[23,24], a scavenger receptor previously implicated in the retention of macrophages in atherosclerosis[22,36]. Macrophages that infiltrate the arterial intima are thought to exit via lymphatic vessels or egress into the bloodstream, or undergo apopotosis and efferocytotic clearance[37-39]. All of these mechanisms appear to be impaired in atherosclerosis, leading to the progressive accumulation of macrophages in plaques. However, recent studies in mouse models suggest

that these processes can be restored with aggressive lipid management, providing hope that atherosclerosis regression can be achieved in humans[40]. Genetic manipulations that reduced plasma non-HDL cholesterol and/or increased HDL cholesterol, promoted macrophage emigration from plaques to regional and systemic lymph nodes via a mechanism involving CCR7, the receptor for CCL19/CCL21[5-9]. Notably, as netrin-1 blocked macrophage chemotaxis to CCL19 and CCL21, it would be expected to inhibit the normal migratory processes that bring about resolution of inflammation. Consistent with this, deletion of netrin-1 in lesional macrophages in $Ldlr^{-/-}$ mice promotes macrophage emigration and reduces plaque size. Although the exact means by which netrin-1 inhibits migration remains to be elucidated, our data indicate that netrin-1 inhibits Rac-mediated re-organization of the actin cytoskeleton, preventing cell spreading and the migration of macrophages out of plaques.

In addition to its effects on macrophages, netrin-1 is a potent chemoattractant for CaSMC, a process dependent on the neogenin receptor. The recruitment of smooth cells by netrin-1 represents a second mechanism by which this guidance molecule could promote atherosclerosis. During plaque progression, the internal elastic lamina can become breached and smooth muscle cells migrate into the intima to participate in lesion growth. In plaques of $Ntn1^{-/-} \rightarrow Ldlr^{-/-}$ chimeric mice, we see a reduction in the accumulation of smooth muscle cells, consistent with the notion that loss of netrin-1 both allows macrophage emigration *from* the plaque, and curtails the recruitment of SMC *into* it. Furthermore, $Ntn1^{-/-} \rightarrow Ldlr^{-/-}$ plaques show fewer apoptotic cells and reduced necrotic area indicating that the mechanisms regulating tissue homeostasis are enhanced in the absence of netrin-1. Together these data underscore the important role that negative guidance cues may play in the persistence of inflammation, and indicate that local inhibition of such factors may have therapeutic value for the resolution of inflammation in atherosclerosis, and other chronic inflammatory diseases.

Supplementary Material

Refer to Web version on PubMed Central for supplementary material.

Acknowledgments

We thank J. Goss and W. Groot for technical support, M. Tessier-Lavigne (Genentech) for $Ntn1^{+/-}$ mice, and T. Kinane (Massachusetts General Hospital) for providing anti-UNC5b antiserum. Support for this work came from the American Heart Association (Grant-in-aid 0655840T to KM; 09POST2080250 to J.vG), National Institutes of Health (RC1HL100815 to KM; R01HL084312 to EF), Heart and Stroke Foundation of Canada (KR), and Conselho Nacional de Desenvolvimento Científico e Tecnológico (01558/2007-6 to LF and JA-L).

APPENDIX

METHODS

Mice

C57BL/6J, $Ldlr^{-/-}$ and $Apoe^{-/-}$ mice were from Charles River Laboratories or Jackson Laboratories. $Ntn1^{+/-}$ mice were a kind gift from M. Tessier-Lavigne (Stanford University) and were backcrossed 8 generations onto a C57BL/6 background. $Cd36^{-/-}$ mice were generated in our laboratory[41]. All mice were maintained in a pathogen-free facility. Experimental procedures were done in accordance with the USDA Animal Welfare Act and the PHS Policy for the Human Care and Use of Laboratory Animals and the Massachusetts General Hospital's and New York University School of Medicine's Subcommittees on Research Animal Care and Use.

Immunohistochemical staining

Human left anterior descending coronary artery segments were obtained from hearts excised at the time of cardiac transplantation, then fixed in neutral buffered formalin and embedded in paraffin. The use of human coronary artery tissue for these studies was approved by the University of Washington Human Subjects Review Committee. Atherosclerotic plaque morphology was determined from 6-μm sections stained with Movat's pentachrome stains. Macrophages were identified using monoclonal antibody HAM-56 (titer: 1:10, DakoCytomation). Rabbit polyclonal antisera were used to identify netrin-1 (titer: 1:500, Calbiochem) or UNC5b (generated by T. B. Kinane against an extracellular domain: SQAGTDSGSEVLPDS)[18] and normal rabbit serum was used as a negative control. Nova red (Vector Laboratories), which yields a red reaction product, was used as the peroxidase substrate and cell nuclei were counterstained with hematoxylin. Macrophages in mouse atherosclerotic lesion were immunostained using rat anti-macrophage antibody (MOMA-2, AbD Serotec), anti-rat HRP-conjugated antibody (AbD Serotec) or control rat IgG2b (AbD Serotec) and DAB Substrate Kit (BD Pharmingen). To detect smooth muscle cells, anti-smooth muscle actin (1A4, AbD Serotec) or mouse IgG2a (DakoCytomation) as a negative control were used together with ARK™ animal research kit peroxidase (DakoCytomation) according to manufacturer's instructions. Cell nuclei were counterstained with hematoxylin (Sigma-Aldrich).

Immunofluorescence staining

Human CaSMCs cultured on glass coverslips were fixed with ice-cold methanol for 4 min at −20°C and blocked with 5% FBS in PBS for 20 min at 22°C. Thereafter, cells were incubated with the indicated primary antibodies for 1 h at 22°C [goat-anti-human neogenin (1 μg/ml, C-20, Santa Cruz Biotechnology), goat-anti-human DCC (4 μg/ml, A-20, Santa Cruz Biotechnology), or normal goat IgG (Santa Cruz Biotechnology)], followed by incubation with a donkey-anti-goat-IgG conjugated to Alexa 488 (Invitrogen). Cells were mounted in Vectashield® mounting medium with DAPI (Vector Laboratories). Images were taken on a Diaphot TMD inverted microscope (Nikon) with a 63x objective and appropriate filters.

Cross-sections of the aortic roots from *Ldlr*$^{-/-}$ mice (5 μm) were fixed with 100% acetone for 10 min and blocked with 4% BSA in PBS. Next, the sections were incubated with the indicated primary antibodies for 2 h at 22°C or overnight at 4°C [rabbit-anti netrin-1 (0.3 μg/ml, ab26162, Abcam), rat-anti-mouse CD68 non-conjugated or conjugated to Alexa 488 (1:300, FA-11, AbD Serotec), rabbit-anti neogenin (1.6 μg/ml, ab26299, Abcam), goat-anti-smooth muscle actin (2.5 μg/ml, ab21027, Abcam)]. Sections were washed and when necessary incubated with biotinylated anti-rabbit-IgG (BA-1000, Vector Laboratories) for 30 min followed by incubation with strepavadin conjugated to Texas Red (Sa-5006, Vector Laboratories), strepavadin conjugated to Fluorescein (Sa-5001, Vector Laboratories), donkey-anti-goat IgG conjugated to Alexa 488 (Invitrogen) or goat-anti-rat IgG conjugated to Alexa 568 (Invitrogen) for 15 min. Sections without primary antibody served as negative controls. The sections were mounted using Vectashield medium with DAPI and visualized using either TCS-SP confocal laser scanning microscope (Leica) or Axioscope 2 Plus fluorescence microscope (Carl Zeiss).

Cell culture

RAW 264.7 and HEK293T cells were obtained from ATCC. Peritoneal macrophages were collected from mice by peritoneal lavage 4 d after intraperitoneal injection with 3% thioglycollate as previously described[41]. Cells were washed in PBS and used for migration or cultured overnight in DMEM (10% FBS) and stimulated for 6-48 h in reduced serum medium (2% FBS) with 50 μg/ml LDL (Biomedical Technologies Inc) or LDL oxidized as

previously described[42]. RNA or protein was isolated as described[42]. Conditioned medium from 4×10^6 cells were collected in 1 ml and concentrated to 250 μl using a centricon YM-30 (Millipore). Human coronary artery smooth muscle cells (Cambrex Bio Sciences) were cultured in growth factor supplemented SmBM.

RT-qPCR

RNA (0.5-1 μg) was reverse transcribed using iScript™ cDNA Synthesis Kit (Biorad) according to manufacturer's instruction. DNA from mouse blood was isolated using ArchivePureTM DNA Kit (5Prime) according to manufacturer's protocol. RT-PCR analysis was conducted using iQ SYBR green Supermix (Biorad) or iTaq Supermix (Biorad) on the iCycler Real-Time Detection System (Biorad). Fold change in mRNA expression was calculated using the comparative cycle method (ΔΔCt). Sequences of primers used are listed in Supplementary table 2.

Immunoblot analysis

Cells were washed in ice-cold PBS and lysed in ice cold RIPA buffer supplemented with 1 mM sodium orthovanadate, 1 mM phenylmethanesulfonylfluoride and 1 mg/ml protease inhibitor cocktail (Roche). 50 μg of protein was separated on a SDS-PAGE gel, transferred to a nitrocellulose or PVDF membrane and blocked in 5% BSA in Tris-buffered saline pH 7.2 containing 0.1% Tween-20 (TBS-T) for 2 hours at 22°C. The membranes were incubated with 1 μg/ml polyclonal rat anti-mouse netrin-1 (158936, R&D Systems) or 0.1 μg/ml phospho-FAK (Tyr576/577, Cell Signaling) overnight at 4°C. Blots were incubated with goat anti-rat horseradish peroxidase-conjugated secondary antibody (1:10,000 dilution, Sigma-Aldrich) or goat anti-rabbit horseradish peroxidase-conjugated secondary antibody (1:2000 dilution, Sigma-Aldrich) for 1 h at 22°C and exposed to ECL reagent (Amersham Biosciences). Signal was recorded using Hyperfilm (Amersham Biosciences). After chemiluminescence detection, memberanes were stripped with 0.2 M NAOH and reprobed with antibodies against α-tubulin (B-5-1-2, Sigma-Aldrich) or FAK (77/FAK, BD Biosciences) for normalization. Densitometry analysis of the gels was carried out using ImageJ software from the NIH (http://rsbweb.nih.gov/ij/).

Netrin-1 ELISA

Detection of netrin-1 by ELISA was performed as previously described[34], with minor modifications. Briefly, 96-well plates (EIA/RIA plate, Corning Incorporated) were coated with 500 ng/well recombinant UNC5b-Fc protein (R&D Systems). Before adding sample, each well was incubated with 350 μl/well of blocking solution, containing 5% (w/v) BSA (Fisher Scientific) in PBS. Standards made with recombinant netrin-1 protein or conditioned medium (250 μl) were added to the coated plates and incubated for 16 h at 4°C plus 2 h at 37°C. After three washes with 0.5% BSA in PBS, 100 μl/well rat anti-netrin-1 (1 μg/ml in 0.5% BSA in PBS, 158936, R&D Systems) was added to each well and incubated for 30 min at 37°C. After extensive washing, each well was incubated with 100 μl/well HRP-conjugated rabbit anti-rat (1:2000 in blocking solution, Sigma-Aldrich) for 30 min at 37°C. After very extensive washing the plates were incubated for up to 20 min at 22°C with 200 μl/well peroxidase substrate solution, *o*-Phenylenediamine dihydrochloride (SIGMAFAST™ OPD tablets, Sigma-Aldrich). The reaction was stopped with 50 μl/well 3M HCl and plate read at 492 nm using a multi-well plate reader (SPECTRAmax M5, Molecular Devices).

Netrin-1 Promoter-Luciferase assay

HEK293T were transfected with a human Netrin-1 promoter luciferase reporter construct (SwitchGear Genomics) using lipofectamineTM 2000 (Invitrogen). After transfection,

media was changed and cells were pretreated with the NF-κB inhibitor BAY 11-7082 (20 μM) for 1 h prior stimulation with 100 μg/ml oxLDL or PBS as a control for 24 h. Luciferase activity was assessed using the Dual-Glo Luciferase Assay System (Promega) and normalized to a constitutively expressed Renilla reporter.

F-actin staining

Freshly isolated peritoneal macrophages were seeded on 8-well LabTek slides (Thermo Scientigfic) for 24 h or used directly. The cells were pretreatment with mouse recombinant netrin-1 (250 ng/ml, R&D Systems) or PBS for 30 min and stimulated with either CCL19 (500 ng/ml, R&D Systems) or CCL2 (10 ng/ml R&D systems) for the indicated times. Macrophages were fixed (4% paraformaldehyde), permeabilized (0.1% Triton X-100) and actin filaments stained with Alexa Fluor 568 or 647 phalloidin (Molecular probes, Invitrogen) at a dilution of 1/40. Cells in suspension were analyzed by flow cytometry (C6 Flow Cytometer, Accuri Cytometers, BD Biosciences). The cells on coverslips were mounted after DAPI staining and vizualized with a Nikon Eclipse microscope and images were captured using the NIS-elements software. Images were background corrected followed by measurement of the average cell area of at least 10 cells per field using the Ivision software.

Rac1 activation assays

Peritoneal macrophages were seeded in a 6-well plate overnight in regular growth media. The cells were stimulated with CCL2 (10 ng/ml R&D systems) for 5 min with or without a pretreatment with mouse recombinant netrin-1 (250 ng/ml, R&D Systems) for 30 min. At the end of stimulation the cells were lysed and Rac1-GTP was measured using Rac1 Activation Assay (Cell Biolabs) according manufacturer's instructions.

Migration assays

Chemotaxis of macrophages (pMø, RAW264.7) and CaSMC was measured in 96-well Boyden chamber with a 5 μm (macrophages) or 8 μm pore size filter (CaSMC) (Neuro Probe) as previously described[18]. Macrophage chemotaxis was also quantified using a Real-time Cell Invasion and Migration (RT-CIM) xCelligence assay system with monitoring every 5 min (Roche Applied Science). Cell migration to CCL2 (100 ng/ml; R&D Systems) or CCL19 (500 ng/ml; R&D Systems) was measured in the absence or presence of recombinant netrin-1 (mouse or chicken from R&D Systems), recombinant rat UNC5b-Fc chimera (cat# 1006-UN, R&D Systems) or whole IgG (Jackson Lab) or conditioned medium from LDL- or oxLDL-stimulated pMø. In some assays, cells were pretreated netrin-1 or UNC5b blocking antibody (AF1006, R&D Systems) or Neogenin blocking antibody (Santa Cruz, sc- 6537) or control goat IgG (Santa Cruz) for 1 h prior to migration. Following cell migration for 3 or 16 h (CaSMC and macrophages, respectively), 4 random high power fields from each well were counted to determine the number of cells that had migrated into the lower chamber. Migration was expressed as chemotactic index, which was calculated by dividing the number of migrating cells in the treated groups by the number of migrating cells in the lowest control well. Results of chemotaxis assays are representative of at least three independent experiments performed on triplicate samples.

In vivo studies of inflammatory leukocyte emigration from the peritoneum

As previously described[22,43], mice (n = 6/group) were injected intraperitoneally with 1 ml of 3% thioglycollate to incite a sterile peritonitis with macrophage numbers peaking on day 4. After 4 d, the mice were pre-treated with netrin-1 (500 ng i.p.) or PBS for 45 min, and then injected with an inflammatory stimulus (400 ng LPS) to induce efflux of leukocytes from the peritoneum to the draining lymph nodes. After 3 h the peritoneal cells were collected by

lavage and counted. The percentage of macrophages in the lavage was quantified by flow cytometry using PE-conjugated anti-F4/80 (CI:A3-1, AbD Serotec).

Fetal liver cell transplantation

Female and male *Ntn1*$^{+/-}$ mice were mated. On day 14 of gestation, embryos were dissected free from the placenta and yolk sac, and a single-cell suspension of fetal liver cell (FLC) was prepared by flushing through graded sizes of needles. Part of the fetal tissues was used for genotyping by X-gal staining intensity, the other part to provide independent confirmation of the genotype by PCR analysis. FLC (2×10^6) were i.v. injected in lethally irradiated *Ldlr*$^{-/-}$ mice, by 2 exposures of 600 cGy. 4 weeks after transplantation, mice were put on a western diet (Teklad Adjusted Calories 88137; 21% (w/w) fat; 0.15% (w/w) cholesterol; 19.5% (w/w) casein, no sodium cholate) for 12 weeks prior to atherosclerosis analysis.

Lipoprotein profile analysis

Pooled plasma from 3 mice per genotype was used to obtain lipoprotein profiles. Profiles were obtained using FLPC gel filtration and Superose 6 column (Amersham Pharmacia), fractions were analyzed for total cholesterol.

Atherosclerotic analysis

After 12 weeks of WD feeding, mice were anesthetized with Tribomoethanol (0.4mg/g i.p.) and ex-sanguinated by cardiac puncture. Plasma was collected from fasted mice and total plasma cholesterol and triglyceride concentrations were measured as described[44]. Aortas were flushed with PBS and perfused with 10% neutral buffered formalin. Aortic roots were embedded in OCT medium, and the aortic arch and descending aorta were placed in formalin overnight. En face lesion analysis was performed on dissected aortas pinned open and imaged with a dissecting microscope. Lesion area was quantified using IP Lab Spectrum software version 3.9 (Scanalytics) and expressed as a percentage of the total aortic area or defined regions. For cross-sectional analysis of lesion area in the aortic root, every second section (5 μm thick) throughout the aortic sinus (400 μm) was taken for analysis and quantified using IP Lab Spectrum software. Lesional necrotic areas were analyzed as we previously described[45], from the average of 6 hematoxylin and eosin stained sections (5 μm thick) per mouse, spaced 25 μm apart. The necrotic area was defined as acellular and anuclear white area and quantified using IP Lab Spectrum software[45]. Apoptotic cells were labeled after proteinase K treatment by TUNEL (TdT-mediated dUTP nick-end labeling) using the in situ cell death detection kit TMR-red (Roche Diagnostics). TUNEL and DAPI staining was viewed using an Zeiss Axioplan Inverted fluorescent microscope and only TUNEL-positive cells that colocalized with DAPI-stained nuclei were counted as being positive.

Labeling and tracking of blood monocytes

Circulating blood monocytes of WT →*Ldlr*$^{-/-}$ and *Ntn1*$^{-/-}$ →*Ldlr*$^{-/-}$ chimeric mice were labeled *in vivo* by retro-orbital i.v. injection of 1 μm Fluoresbrite green fluorescent (YG) plain microspheres (Polysciences) diluted 1:4 in sterile PBS as previously described by us and others[7,8,26]. This method predominantly labels Ly6c^{lo} monocytes and labeling efficiency (% beads positive blood monocytes) was measured by flow cytometry 1 d after injection of beads. One group of mice was harvested after 72 h for baseline measurements, as this time point has previously been shown to have optimal recruitment of labeled monocytes to atherosclerotic plaques and clearance of the labeled monocytes from the blood. A second group of mice was harvested 14 d later to measure the number of labeled macrophages remaining in plaques. The number of beads per section were normalized for the monocyte labeling efficiency by multiplying the mean number of beads per section of

mouse A by the % bead positive blood monocytes of all mice/mouse A as previously described. Over time, the bead content of the plaque will decrease if the beads left in the same cells that brought them in or if they were transferred to another monocyte-derived cell that then left. In other words, a decrease in bead number indicates that there was emigration of monocyte-derived cells from the plaque.

Statistics

The difference between two groups was analyzed by Student's t-test or by one-way ANOVA followed by the Newman-Keuls multiple comparison test. A *P*-value of <0.05 was considered significant.

REFERENCES

1. Moore KJ, Tabas I. Macrophage in the pathogenesis of atherosclerosis. Cell. 2011; 145:341–355. [PubMed: 21529710]
2. Libby P, Aikawa M. Stabilization of atherosclerotic plaques: new mechanisms and clinical targets. Nat Med. 2002; 8:1257–1262. [PubMed: 12411953]
3. Bellingan GJ, Caldwell H, Howie SE, Dransfield I, Haslett C. In vivo fate of the inflammatory macrophage during the resolution of inflammation: inflammatory macrophages do not die locally, but emigrate to the draining lymph nodes. J Immunol. 1996; 157:2577–2585. [PubMed: 8805660]
4. Randolph GJ. Emigration of monocyte-derived cells to lymph nodes during resolution of inflammation and its failure in atherosclerosis. Curr Opin Lipidol. 2008; 19:462–468. [PubMed: 18769227]
5. Rong JX, et al. Elevating high-density lipoprotein cholesterol in apolipoprotein E-deficient mice remodels advanced atherosclerotic lesions by decreasing macrophage and increasing smooth muscle cell content. Circulation. 2001; 104:2447–2452. [PubMed: 11705823]
6. Llodra J, et al. Emigration of monocyte-derived cells from atherosclerotic lesions characterizes regressive, but not progressive, plaques. Proc Natl Acad Sci U S A. 2004; 101:11779–11784. [PubMed: 15280540]
7. Feig JE, et al. Reversal of hyperlipidemia with a genetic switch favorably affects the content and inflammatory state of macrophages in atherosclerotic plaques. Circulation. 2011; 123:989–998. [PubMed: 21339485]
8. Feig JE, et al. LXR promotes the maximal egress of monocyte-derived cells from mouse aortic plaques during atherosclerosis regression. J Clin Invest. 2010; 120:4415–4424. [PubMed: 21041949]
9. Trogan E, et al. Gene expression changes in foam cells and the role of chemokine receptor CCR7 during atherosclerosis regression in ApoE-deficient mice. Proc Natl Acad Sci U S A. 2006; 103:3781–3786. [PubMed: 16537455]
10. Cirulli V, Yebra M. Netrins: beyond the brain. Nat Rev Mol Cell Biol. 2007; 8:296–306. [PubMed: 17356579]
11. Keleman K, Dickson BJ. Short- and long-range repulsion by the Drosophila Unc5 netrin receptor. Neuron. 2001; 32:605–617. [PubMed: 11719202]
12. Srinivasan K, Strickland P, Valdes A, Shin GC, Hinck L. Netrin-1/neogenin interaction stabilizes multipotent progenitor cap cells during mammary gland morphogenesis. Dev Cell. 2003; 4:371–382. [PubMed: 12636918]
13. Salminen M, Meyer BI, Bober E, Gruss P. Netrin 1 is required for semicircular canal formation in the mouse inner ear. Development. 2000; 127:13–22. [PubMed: 10654596]
14. Nguyen A, Cai H. Netrin-1 induces angiogenesis via a DCC-dependent ERK1/2-eNOS feed-forward mechanism. Proc Natl Acad Sci U S A. 2006; 103:6530–6535. [PubMed: 16611730]
15. Wilson BD, et al. Netrins promote developmental and therapeutic angiogenesis. Science. 2006; 313:640–644. [PubMed: 16809490]
16. Arakawa H. Netrin-1 and its receptors in tumorigenesis. Nat Rev Cancer. 2004; 4:978–987. [PubMed: 15573119]

17. Fitamant J, et al. Netrin-1 expression confers a selective advantage for tumor cell survival in metastatic breast cancer. Proc Natl Acad Sci U S A. 2008; 105:4850–4855. [PubMed: 18353983]
18. Ly NP, et al. Netrin-1 inhibits leukocyte migration in vitro and in vivo. Proc Natl Acad Sci U S A. 2005; 102:14729–14734. [PubMed: 16203981]
19. Mirakaj V, et al. Netrin-1 dampens pulmonary inflammation during acute lung injury. Am J Respir Crit Care Med. 2010; 181:815–824. [PubMed: 20075388]
20. Rosenberger P, et al. Hypoxia-inducible factor-dependent induction of netrin-1 dampens inflammation caused by hypoxia. Nat Immunol. 2009; 10:195–202. [PubMed: 19122655]
21. Wang W, Reeves WB, Ramesh G. Netrin-1 and kidney injury. I. Netrin-1 protects against ischemia-reperfusion injury of the kidney. Am J Physiol Renal Physiol. 2008; 294:F739–747. [PubMed: 18216145]
22. Park YM, Febbraio M, Silverstein RL. CD36 modulates migration of mouse and human macrophages in response to oxidized LDL and may contribute to macrophage trapping in the arterial intima. J Clin Invest. 2009; 119:136–145. [PubMed: 19065049]
23. Janabi M, et al. Oxidized LDL-induced NF-kappa B activation and subsequent expression of proinflammatory genes are defective in monocyte-derived macrophages from CD36-deficient patients. Arterioscler Thromb Vasc Biol. 2000; 20:1953–1960. [PubMed: 10938017]
24. Stewart CR, et al. CD36 ligands promote sterile inflammation through assembly of a Toll-like receptor 4 and 6 heterodimer. Nat Immunol. 2010; 11:155–161. [PubMed: 20037584]
25. Bellingan GJ, et al. Adhesion molecule-dependent mechanisms regulate the rate of macrophage clearance during the resolution of peritoneal inflammation. The Journal of experimental medicine. 2002; 196:1515–1521. [PubMed: 12461086]
26. Tacke F, et al. Monocyte subsets differentially employ CCR2, CCR5, and CX3CR1 to accumulate within atherosclerotic plaques. The Journal of clinical investigation. 2007; 117:185–194. [PubMed: 17200718]
27. Sato N, et al. CC chemokine receptor (CCR)2 is required for langerhans cell migration and localization of T helper cell type 1 (Th1)-inducing dendritic cells. Absence of CCR2 shifts the Leishmania major-resistant phenotype to a susceptible state dominated by Th2 cytokines, b cell outgrowth, and sustained neutrophilic inflammation. The Journal of experimental medicine. 2000; 192:205–218. [PubMed: 10899907]
28. Jimenez F, et al. CCR2 plays a critical role in dendritic cell maturation: possible role of CCL2 and NF-kappa B. Journal of immunology. 2010; 184:5571–5581.
29. Delaire S, et al. Biological activity of soluble CD100. II. Soluble CD100, similarly to H-SemaIII, inhibits immune cell migration. J Immunol. 2001; 166:4348, 4354. [PubMed: 11254688]
30. Munoz JJ, et al. Expression and function of the Eph A receptors and their ligands ephrins A in the rat thymus. J Immunol. 2002; 169:177–184. [PubMed: 12077243]
31. Wu JY, et al. The neuronal repellent Slit inhibits leukocyte chemotaxis induced by chemotactic factors. Nature. 2001; 410:948–952. [PubMed: 11309622]
32. Wang W, Reeves WB, Pays L, Mehlen P, Ramesh G. Netrin-1 overexpression protects kidney from ischemia reperfusion injury by suppressing apoptosis. Am J Pathol. 2009; 175:1010–1018. [PubMed: 19700747]
33. Khan JA, et al. Systemic human Netrin-1 gene delivery by adeno-associated virus type 8 alters leukocyte accumulation and atherogenesis in vivo. Gene Ther. 2010
34. Paradisi A, et al. NF-kappaB regulates netrin-1 expression and affects the conditional tumor suppressive activity of the netrin-1 receptors. Gastroenterology. 2008; 135:1248–1257. [PubMed: 18692059]
35. Parathath S, et al. Hypoxia is present in murine atherosclerotic plaques and has multiple adverse effects on macrophage lipid metabolism. Circulation research. 2011; 109:1141–1152. [PubMed: 21921268]
36. Curtiss LK. Reversing atherosclerosis? N Engl J Med. 2009; 360:1144–1146. [PubMed: 19279347]
37. Gerrity RG. The role of the monocyte in atherogenesis: II. Migration of foam cells from atherosclerotic lesions. Am J Pathol. 1981; 103:191–200. [PubMed: 7234962]

38. Kling D, Holzschuh T, Betz E. Recruitment and dynamics of leukocytes in the formation of arterial intimal thickening--a comparative study with normo- and hypercholesterolemic rabbits. Atherosclerosis. 1993; 101:79–96. [PubMed: 8216505]

39. Landers SC, Gupta M, Lewis JC. Ultrastructural localization of tissue factor on monocyte-derived macrophages and macrophage foam cells associated with atherosclerotic lesions. Virchows Arch. 1994; 425:49–54. [PubMed: 7921413]

40. Williams KJ, Feig JE, Fisher EA. Rapid regression of atherosclerosis: insights from the clinical and experimental literature. Nature clinical practice. Cardiovascular medicine. 2008; 5:91–102.

41. Moore KJ, et al. A CD36-initiated signaling cascade mediates inflammatory effects of beta-amyloid. J Biol Chem. 2002; 277:47373–47379. [PubMed: 12239221]

42. Kunjathoor VV, et al. Scavenger receptors class A-I/II and CD36 are the principal receptors responsible for the uptake of modified low density lipoprotein leading to lipid loading in macrophages. J Biol Chem. 2002; 277:49982–49988. [PubMed: 12376530]

43. Cao C, Lawrence DA, Strickland DK, Zhang L. A specific role of integrin Mac-1 in accelerated macrophage efflux to the lymphatics. Blood. 2005; 106:3234–3241. [PubMed: 16002427]

44. Moore KJ, et al. Loss of receptor-mediated lipid uptake via scavenger receptor A or CD36 pathways does not ameliorate atherosclerosis in hyperlipidemic mice. J Clin Invest. 2005; 115:2192–2201. [PubMed: 16075060]

45. Manning-Tobin JJ, et al. Loss of SR-A and CD36 activity reduces atherosclerotic lesion complexity without abrogating foam cell formation in hyperlipidemic mice. Arterioscler Thromb Vasc Biol. 2009; 29:19–26. [PubMed: 18948635]

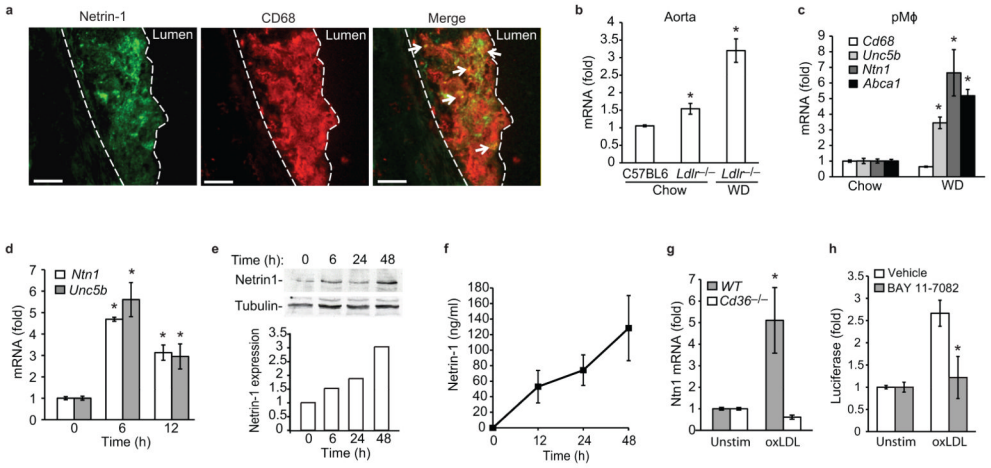

Figure 1. Netrin-1 and it receptor UNC5b are abundantly expressed by macrophage foam cells in atherosclerotic lesions

(**a**) Immunofluorescent staining of netrin-1 (green) and CD68 (red), and their colocalization (yellow, arrows), in aortic sinus atherosclerotic plaques of *Ldlr*$^{-/-}$ mice fed a WD. Dashed line indicates lesion border (scale bar= 50 μm). Staining is representative of plaques from 4 mice. (**b**) qPCR analysis of *Ntn1* mRNA isolated from the aortic arch of C57BL/6 or *Ldlr*$^{-/-}$ mice fed a chow or WD. (**c**) qPCR analysis of *Ntn1, Unc5b, Cd68* and *Abca1* mRNA in pMø isolated from *Ldlr*$^{-/-}$ mice fed a chow or WD. (**d**) qPCR analysis of *Ntn1* and *Unc5b* in pMø treated with 50 μg/ml oxLDL, and corresponding expression of netrin-1 protein measured in (**e**) cell lysates by immunoblot or (**f**) conditioned media by ELISA. (**g**) qPCR analysis of *Ntn1* mRNA in wild-type (WT) or *Cd36*$^{-/-}$ pMø stimulated with 50 μg/ml oxLDL for 6 h. (**h**) *Ntn1* promoter-luciferase reporter activity in HEK293 cells treated with oxLDL in the presence or absence of the NF-κB inhibitor BAY 11-7082 (20 μM). (**b-h**) Data are mean ± s.d. of triplicate samples in a single experiment and are representative of 3 independent experiments. **P*<0.05.

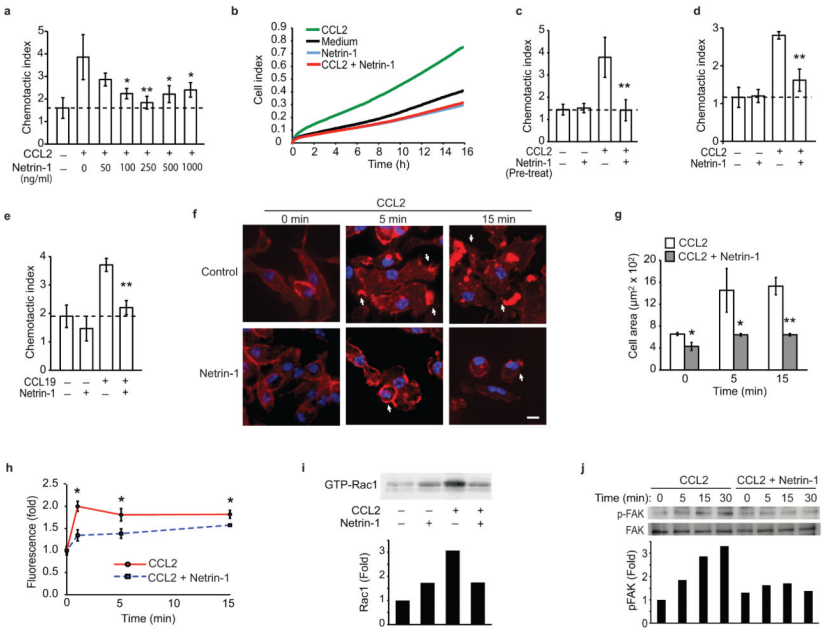

Figure 2. Netrin-1 inhibits macrophage migration to CCL2 and CCL19, via its receptor UNC5b

(**a**) Migration of RAW264.7 cells to CCL2 (100 ng/ml) was measured in the absence or presence of increasing concentrations of recombinant netrin-1 placed in the lower compartment of a Boyden chamber. (**b**) Real-time measurement of migration of RAW264.7 cells to 250 ng/ml netrin-1, 100 ng/ml CCL2, or both. (**c**) Migration of RAW264.7 cells pretreated (PT) with 250 ng/ml netrin-1 and exposured to CCL2 (100 ng/ml). (**d-e**) Migration of mouse pMø to (**d**) CCL2 (100 ng/ml) or (**e**) CCL19 (500 ng/ml), in the absence/presence of 250 ng/ml netrin-1. (**f**) pMø stained with phalloidin to detect polymerized actin after treatment with 100 ng/ml CCL2 with or without 250 ng/ml netrin-1. Arrows indicate membrane ruffles, scale bar 10 μm. (**g**) Mean cell surface area of pMø in (f). (**h**). Quantification of actin polymerization by flow cytometric analysis of phallodin staining. (**i**) Amount of activated Rac1 in pMø treated for 5 min with 100 ng/ml CCL2 with and without 250 ng/ml netrin-1. (**j**) Immunoblot of phospho- and total FAK in pMø incubated with 100 ng/ml CCL2 with or without 250 ng/ml netrin-1 pretreatment. Data are the mean ± s.d. of triplicate samples in a single experiment and are representative of 3 independent experiments. $P < 0.05$, $^{**}P < 0.01$.

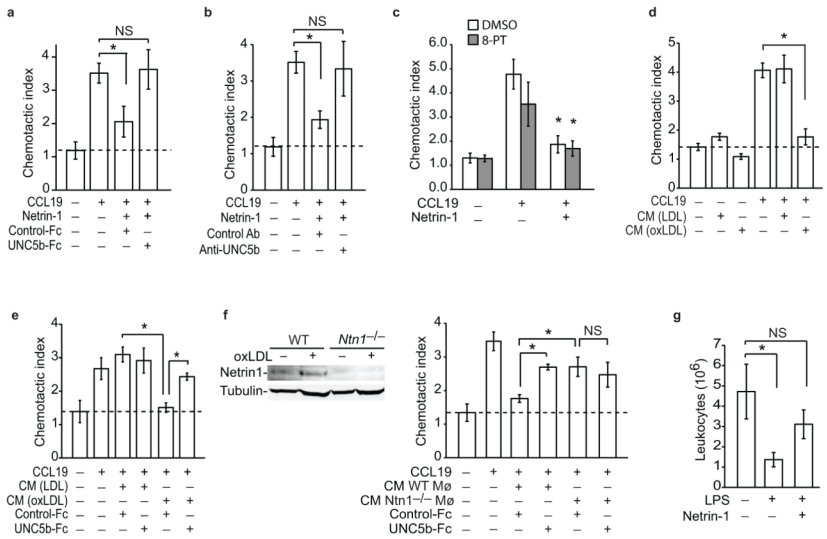

Figure 3. Foam cell secreted netrin-1 blocks macrophage migration

(**a-c**) Migration of pMø to CCL19 (500 ng/ml) with/without netrin-1 (250 ng/ml) in the presence of (**a**) recombinant UNC5b-Fc or IgG control, (**b**) anti-UNC5b or isotype-matched control antibody, or (**c**) an inhibitor of the A2B adenosine receptor (10 uM 8-PT). **(d-e)** Migration of pMø to CCL19 (500 ng/ml) in (**d**) the presence or absence of conditioned medium (CM) from macrophages treated with LDL or oxLDL (50 μg/ml; 48 h) and (**e**) with/without recombinant UNC5b-Fc or IgG control. (**f**) Migration of pMø to CCL19 (500 ng/ml) as in (**e**) except using conditioned medium (CM) from WT or *Ntn1*$^{-/-}$ macrophages treated with oxLDL. Inset: immunoblot of netrin-1 in lysates of WT and *Ntn1*$^{-/-}$ pMø. **(a-f)** Data are the mean ± s.d. of triplicate samples in a single experiment and are representative of 3 independent experiments. *$P < 0.01$. (**g**) Effect of netrin-1 (500ng) or PBS pretreatment on LPS-induced leukocyte emigration from the peritoneum of mice with established thioglycollate-induced peritonitis. Data are the mean number (± s.e.m) of leukocytes in the peritoneum of mice (n = 6/group) before and 4h after injection of 400ng LPS ip., and are representative of 2 independent experiments. *$P < 0.05$.

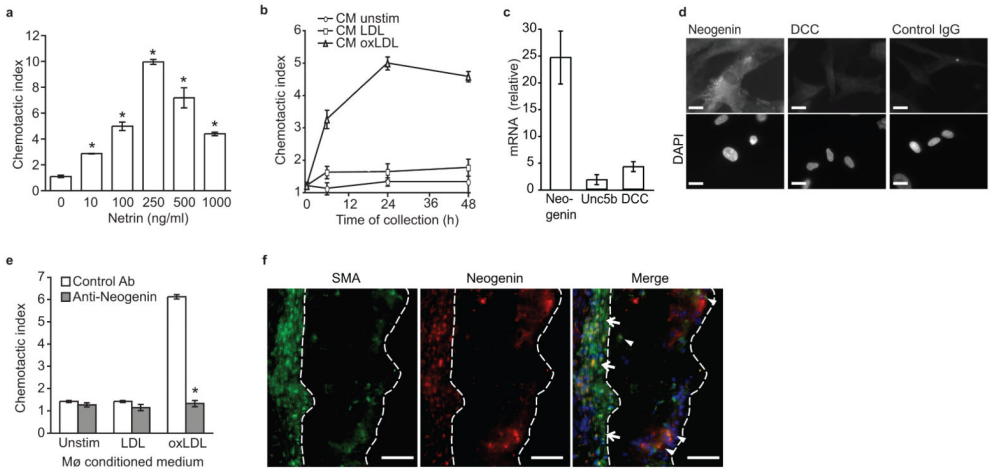

Figure 4. Netrin-1 acts as a chemoattractant for smooth muscle cells via the receptor neogenin

(**a**) Migration of human CaSMCs in the presence of recombinant netrin-1. (**b**) Migration of CaSMCs in the presence of conditioned media from macrophages treated for the indicated times with LDL or oxLDL (50 μg/ml). (**c**) qPCR analysis of *Neogenin, Unc5b* and *Dcc* mRNAs in CaSMC. (**d**) Immunofluorescent staining for neogenin, DCC or isotype-matched control antibody in CaSMCs. Cells were co-stained with DAPI nuclear stain. Scale bar, 10 μm. (**e**) Migration of CaSMCs pre-treated with neogenin or isotype control antibody prior to exposure to conditioned media from macrophages treated as indicated for 24 h. (**f**) Immunofluorescent staining of alpha smooth muscle actin (SMA, green), neogenin (red) and DAPI (blue) in atherosclerotic plaques of $Ldlr^{-/-}$ mice fed a WD. Co-localization of SMA and neogenin (yellow in the merged image) was detected in the media (arrows) and in SMC that had invaded the intima (arrowheads). Staining is representative of plaques from 5 mice. Scale bar, 50 μm. (**a-c, e**) Data are the mean ± s.d. of triplicate samples in a single experiment and are representative of 3 independent experiments. $*P < 0.05$.

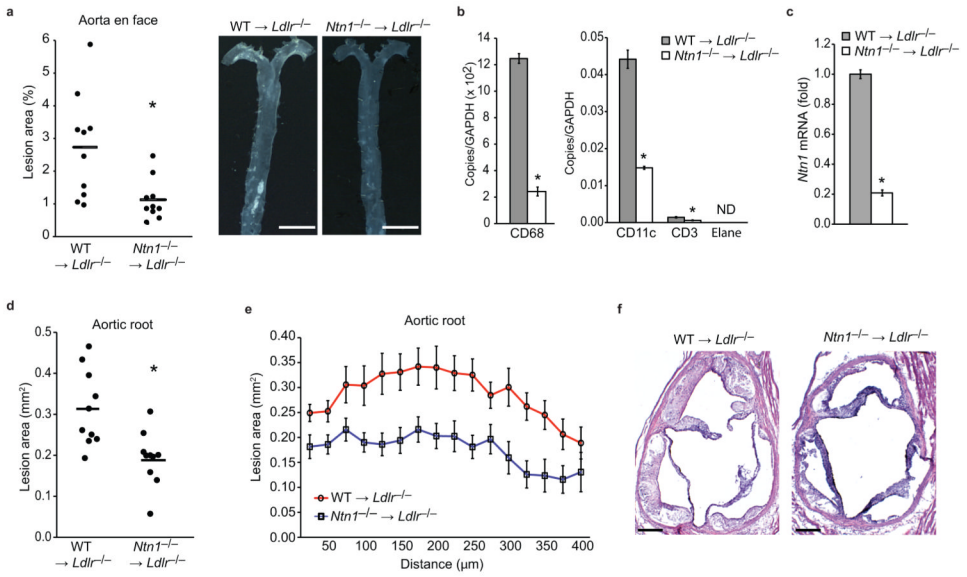

Figure 5. Targeted deletion of netrin-1 in immune cells reduces atherosclerosis burden

(**a**) Quantification and representative photographs of atherosclerosis in the aorta *en face* of *WT→Ldlr*$^{-/-}$ and *Ntn1*$^{-/-}$*→Ldlr*$^{-/-}$ chimeric mice (n=10/group). *$P < 0.01$. Scale bar, 5 mm. (**b-c**) qPCR analysis of *Cd68* (macrophage), *Cd3* (T cell), *Cd11c* (dendritic cell), *Elane* (neutrophil) and *Ntn1* mRNA in the aortic arches of *WT→Ldlr*$^{-/-}$ and *Ntn1*$^{-/-}$*→Ldlr*$^{-/-}$ chimeric mice (n=3/group). Data are the mean ± s.d. of triplicate samples in a single experiment and are representative of 2 independent experiments. *$P < 0.05$. (**d-e**) Lesion area of atherosclerotic plaques of the aortic root of *WT→Ldlr*$^{-/-}$ and *Ntn1*$^{-/-}$*→Ldlr*$^{-/-}$ mice expressed as the mean (**d**) of individual mice and (**e**) of each genotype across the 400 μm of the aortic root. *$P < 0.005$. (**f**) Representative photographs of hematoxylin and eosin stained aortic sinus lesions of *WT→Ldlr*$^{-/-}$ and *Ntn1*$^{-/-}$*→Ldlr*$^{-/-}$ mice. Scale bar, 200 μm.

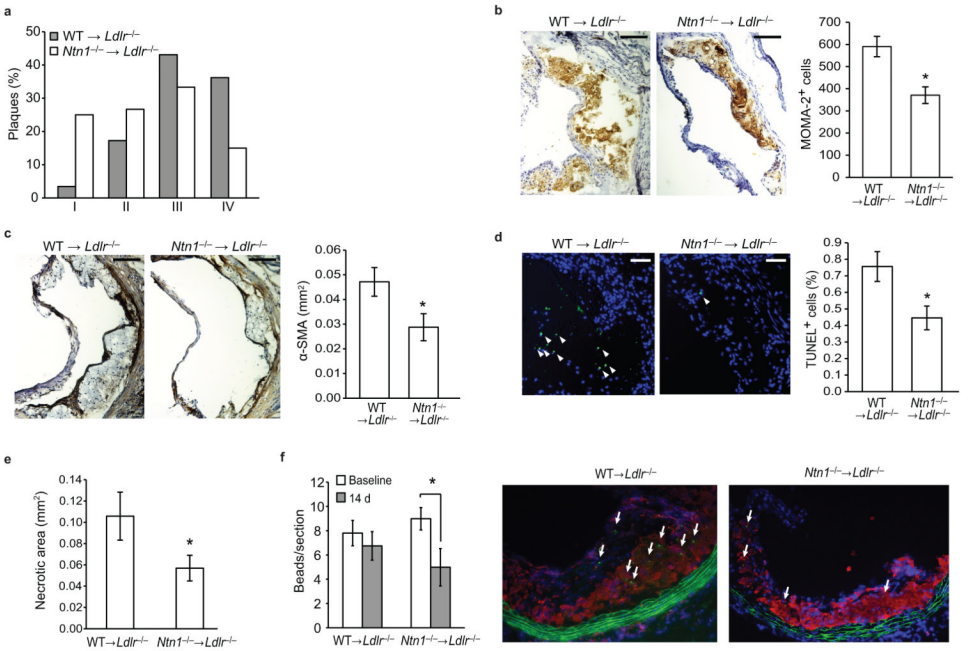

Figure 6. Targeted deletion of netrin-1 in immune cells reduces plaque complexity and promotes macrophage emigration

(**a**) Classification of aortic sinus plaques of $WT \rightarrow Ldlr^{-/-}$ and $Ntn1^{-/-} \rightarrow Ldlr^{-/-}$ mice (n = 10) according to the Stary method. I. Early (foam cells), II. Moderate 1 (foam cells, SMC), III. Moderate 2 (foam cells, SMC, clefts), IV. Advanced (necrotic core). (**b,c**) Immunohistochemical staining of aortic sinus plaques for (**b**) macrophages (MOMA-2) and (**c**) SMC (α-smooth muscle actin). Scale bar, 100 μm. Staining quantified using IP Lab Spectrum software is presented at right. n = 6-9. (**d**) Immunofluorescent staining of apoptotic cells (green) in aortic sinus plaques. TUNEL positive nuclei are indicated by arrowheads TUNEL and quantification is presented at right. Scale bar, 50 μm. n = 9. (**e**) Quantification of necrotic areas of aortic sinus plaques. n = 10. *P = 0.07. (**f**) *In vivo* analysis of macrophage recruitment and retention in atherosclerotic plaques of $WT \rightarrow Ldlr^{-/-}$ and $Ntn1^{-/-} \rightarrow Ldlr^{-/-}$mice using a monocyte bead-tracking model. The mean number of bead-labeled macrophages per plaque is shown 3 days (baseline) and 14 days after monocyte labeling (n = 3-4/group). . Representative image of plaques stained for CD68 (red) and cell nuclei (blue). Arrows indicate the presence of the cells containing fluorescent beads (green) within the lesion. Data in a-f are the mean ± s.e.m., *P < 0.05, unless otherwise noted.